Er3+ and Ce3+ Co-Doped Tellurite Optical Fiber for Lasers And Amplifiers in the Near Infrared Wavelength Region: Fabrication, Optical Characterization and Prospects

Er^{3+} and Ce^{3+} Co-Doped Tellurite Optical Fiber for Lasers And Amplifiers in the Near Infrared Wavelength Region: Fabrication, Optical Characterization and Prospects

J. Lousteau,[1] N. Boetti,[1] A. Chiasera,[2] M. Ferrari,[2] S. Abrate,[3] Member, IEEE, G. Scarciglia,[3] A. Venturello,[1] D. Milanese[1]

[1] PhotonLab, Dipartimento di Scienza dei Materiali ed Ingegneria Chimica, Politecnico di Torino, Via P. Boggio 61 10134 Torino, Italy.

[2] CNR-IFN, Istituto di Fotonica e Nanotecnologie, CSMFO Lab. via alla Cascata 56/C, Povo, 38123, Trento, Italy.

[3] Istituto Superiore Mario Boella, Via P. Boggio 61, 10134 Torino, Italy.

This research was sponsored by Regione Piemonte (Italy) through the Converging Technologies research project "Hipernano".

Abstract.

A tellurite optical fiber doped with Er3+ and Ce3+ ions was designed and fabricated with the aim of assessing its suitability as laser and optical amplifier operating at 1550 nm and compatible with silica fiber standard dimensions. High quality optical fibers, with an attenuation loss of 1.0 dB/m at 1320 nm, were obtained featuring a 6 □m diameter core. A fiber laser emitting at 1550 nm upon pumping at 976 nm and a fiber amplifier characterized by signal amplification of 8 dB for a length of 10 cm were demonstrated.

Index Terms: Oxide materials, Fiber lasers, Laser amplifiers.

1. Introduction

With the increasing need for telecom bandwidth, the development of novel optical amplifiers offering wider gain bandwidth than current technologies remains a research topic of prime interest. Current amplifier technology relies for most and for all on Erbium Doped Fiber Amplifiers (EDFA) made from silica glass fibers, whose typical gain bandwidth is tens of nanometers in the C-band [1].

Tellurite glass is one of the materials whose physical properties could allow to supplant silica glass for amplifier components. Tellurite glasses have a wide transmission region (0.35–5 μm), good glass stability and corrosion resistance, the lowest vibrational energy (about 780 cm^{-1}) among oxide glass formers, low process temperature, and a high refractive index which increases the local field correction at the rare-earth ion site and leads to an enhancement of the radiative transition rates [2, 3, 4]. Er-doped tellurite glasses offer high and very broadband emission cross sections in the third telecom window [5,6] thus have been proposed as an alternative for high density optical networks. Through a series of publications [7,8,9] the research group at Nippon Telecom did report the demonstration of a 14 m long erbium doped tellurite glass fiber amplifier reaching a maximum small signal gain up to 50 dB and a 20 dB small signal gain across a 80 nm bandwidth. However, despite the very promising results reported by the NTT research group, Er^{3+} doped tellurite glass optical fibers have not yet been exploited in the form of commercial devices operating at standard telecom wavelength.

To understand the possible reasons behind this lack of exploitation, we have fabricated an Er/Ce doped tellurite glass fiber that we have implemented as an optical amplifier operating in the third telecom window.

In this article we review the range of performances achievable using this type of fiber and discuss its possible limitations not only in terms of optical performances but also in terms of manufacturing/packaging effort required to develop a reliable component.

2. Experimental Details

2.1. Glass and fiber fabrication and characterization

The glass fiber was made out of three different glass compositions, namely TZ1 (outer cladding), TZ2 (inner cladding) and TZ3 (core). The details of the glass compositions are given in Table 1. The choice of a double cladding structure was driven to ensure a uniform collapse around the structured central rod during fiber drawing. The core glass TZ3 was doped with 0.5 wt% of Er_2O_3 ($8.12 \cdot 10^{19}$ Er^{3+} ions per cm^3) and 1 wt % of CeO_2, corresponding to a concentration in either Ce^{3+} or Ce^{4+} ions of $1.92 \cdot 10^{19}$ per cm^3.

The introduction of CeO_2 as a co-dopant follows the successful demonstration [10] of a more efficient emission from Er^{3+} when co doped with Ce^{3+}. Actually, in low phonon energy material such as tellurite glasses the relatively long lifetime of level $^4I_{11/2}$ results in enhanced excited state absorption (ESA) resulting in green upconversion emission rather than the targeted emission centered in the telecom window around 1.5 μm. As reported in [11,12] the introduction of Ce^{3+} has for effect to enhance the non radiative transition of Er^{3+} from $^4I_{11/2}$ towards the $^4I_{13/2}$ level.

The doping concentration was kept to a moderate level in order to avoid any detrimental effect such as ion clustering and other possible concentration quenching phenomena [13,14,15]. The minimum purity of the chemical precursors involved in this work was 99+%. After weighting and mixing, the batched chemicals were transferred into a platinum crucible for melting within a chamber furnace. The melting procedure was carried out inside a glove box under dried air atmosphere with a water level lower than 1 ppm. The onset melting temperature was 730 ˚C and the duration of the process 2 hours. The melt was cast in a brass mold preheated to 300 ˚C and annealed at T_g – 10 ˚C for 2 h.

Thermal analysis was performed on fabricated glasses using a Perkin Elmer DSC-7 differential scanning calorimeter up to 550°C under Ar flow with a heat rate of 10°C/min in sealed Al pans using around 30 mg glass samples. Thermal analysis was carried out to measure the characteristic temperatures T_g (glass transition temperature) and T_x (onset crystallization temperature). Their measurement also allows assessing the corresponding glass stability. These temperatures were measured with an error of ±3°C. The refractive index of the glasses was measured at 1.3 μm by prism coupling technique (Metricon, model 2010). The resolution of the instrument was ± 0.0001. Absorption spectra in the IR region were also measured in order to assess the occurrence of Ce^{3+} ions, as explained below in the discussion. Such measurements were carried out on a 2 mm thick sample optically polished on both sides. Fourier transform infrared spectrometer (Bruker, Tensor 27) working in transmission mode, equipped with DTGS detector, was employed and the spectra were acquired with OPUS 6.5 acquisition software. Spectra have been taken between 6000 and 400 cm^{-1} with a resolution of 4 cm^{-1} and acquiring an average of 64 scans. A cerium free tellurite glass with very similar composition ($79TeO_2$:$13ZnO$:$8Na_2O$ + 0.5 wt% Er_2O_3) was used as reference to compare the spectral features.

The optical fiber preform was produced by the built-in-casting technique. For this process the TZ2 and TZ3 glasses went through a second melting step which had to be carried out in laboratory atmosphere to ease the casting procedure. The jacketing cladding tube was produced from glass TZ1 by the rotational casting technique at a rotational speed of 3000 rpm. Dimensions of the obtained tube were 11 mm outer diameter (OD), 3.8 mm inner diameter (ID) and 120 mm in length. The core/clad structured rod produced by built-in-casting was stretched down to a diameter of 3.5 mm to fit into the jacketing tube.

The preform was drawn into fiber using a drawing tower developed in-house. The furnace consists in a graphite ring heated by an induction operating at 248 kHz and delivering 170 W to reach drawing temperature (SAET, Torino, Italy). The preform was fed into the furnace and drawn into fiber at speed of 2.5 m/min under a tension of 70 mN. About 150 m of fiber were manufactured. The diameter of the fiber was monitored and recorded during drawing using an optical diameter monitor and by recording the online data using a personal computer.

Preform and fiber fabrications parameters were set in order to develop a fiber with a core of 6 μm diameter. Such value was targeted to achieve an acceptable coupling efficiency from the flexcore fiber (5.6 μm core diameter) while limiting the multimodal behavior arising from the large numerical aperture (see section 3). Moreover, the use of a larger core with respect to previous work allows using shorter length of fiber for reaching the same amplification level. This is an important issue if one considers the development of compact component and the difficulties in managing long length of tellurite glass fiber due to the fragility of the material itself.

The fabricated optical fiber was inspected for quality and morphology by means of optical microscopy using a Nikon ECLIPSE E 50i microscope. The attenuation of the fiber was measured by the cut-back method using a single mode optical fiber laser diode at 1.29 μm for three sections of fiber corresponding to the initial, central and final stages of the drawing process. The modal properties of the fiber were analyzed by near-field imaging the output of a 7 m long section of fiber at the wavelength of 1.29 μm by butt coupling a fiber pigtailed single mode laser diode.

An additional glass pair was fabricated to compare the effect of Cerium addition on the optical properties of the TZN glass. These glasses featured the same host composition ($79TeO_2$:13ZnO:$8Na_2O$). TZ4 was doped 0.5 wt%Er_2O_3 while TZ5 was doped with 0.5 wt% Er_2O_3 + 1 wt% CeO_2. Glass synthesis was carried out under dry atmosphere in a glove box in order to minimize the OH content.TZ5 glass shared the same composition of TZ3, which involved a fabrication step in laboratory atmosphere. However, to be compared rigorously with TZ4, TZ5 was entirely manufactured in the controlled glove box environment in order to minimize the OH content.

2.1. Laser and gain experiments

A 10 cm long section of tellurite glass fiber was used to demonstrate laser emission at the wavelength of 1.55 μm. The optical fiber was pumped at 976 nm by butt coupling a fiber pigtailed single mode laser diode (Pirelli model 23041). The laser cavity relied on the Fresnel reflections occurring at the fiber end facets. For the tellurite glass considered in this work the Fresnel reflection coefficient was 12 %, thus providing sufficient feedback to allow for lasing. Although this configuration does not allow for stable lasing operation in terms of operating wavelength, this could be achieved through further optimization, which is out of the scope of this paper. In silica glass fiber, pumping at this wavelength allows obtaining higher gain per unit length and lower noise than pumping schemes at other wavelengths such as 1480 nm [16]. The collected signal was sent to an optical spectrum analyzer (OSA). The laser output power was recorded with respect to pumping power in order to determine the laser slope efficiency.

Another section of the same fiber was deployed to operate as an optical amplifier. The experimental setup consisted of a length of fiber that was butt-coupled at one end, to a Flexcore 1060 optical fiber supplying the optical signal generated by a tunable laser and at the other end, to a wavelength division multiplexer (WDM) also using Flexcore 1060 fiber. The WDM was itself connected to ~~a~~ the 976 nm laser diode delivering 100 mW of optical pump power into the tellurite glass fiber in a counter-propagating fashion. The output of the WDM was connected to an optical spectrum analyzer where the amplitude of the amplified signal could be measured.

2.1. Fluorescence spectroscopy and lifetime measurements

The two samples TZ4 and TZ5 were tested for fluorescence by pumping them at the wavelengths of 795 nm, using a single mode fiber pigtailed laser diode (QPhotonics QFLD-795-100S) with a power of 100 mW, and at 514.5 nm by an Ar ion laser with a power on the sample of 0.5 mW. The NIR luminescence was dispersed by a 320 mm single-grating monochromator with a resolution of 2 nm. The light was detected using a Hamamatsu photomultiplier tube (PMT R943-

02) and a Hamamatsu P4631-02 (IR light) and standard lock-in technique. Decay curves were obtained by chopping the 514.5 nm CW exciting beam with a mechanical chopper and recording the emitted signal with a digital oscilloscope. In the case of 795 nm excitation the diode power supply was triggered by a wave generator. All the measurements were performed at room temperature. Fluorescence spectra and lifetime measurements were collected in both wavelength regions by exciting the samples at the very edge in order to minimize re-absorption.

3. Results

3.1. Glass and fibre characterization

Thermal analysis and refractive index measurements of the optical fiber glass precursors are reported in Table 1.

TABLE 1

Composition, glass transition temperature T_g, onset crystallization temperature T_x, $\Delta T = T_x - T_g$, and refractive index at 1321 nm for the tellurite glasses synthesized to fabricate the optical fiber. Doping values of rare earth ions are expressed in added wt% with respect to the host material.

Glass name	Composition (mol%)	T_g (°C) ± 3 °C	T_x (°C) ± 3 °C	ΔT (°C) ± 6 °C	n at 1321 nm ± 0.0001
TZ1	$75TeO_2$:15ZnO:$10Na_2O$	287	398	111	1.949
TZ2	76 TeO_2:15ZnO:9 Na_2O	292	404	112	1.959
TZ3	$79TeO_2$:13ZnO:$8Na_2O$ + 0.5 wt% Er_2O_3 +1 wt % CeO_2	296	434	138	1.985

It is possible to observe that the fiber glass compositions showed an increasing value of the T_g going from the outer cladding towards the core. The same observation can be made for the crystallization temperature and for the glass stability against crystallization. This configuration guarantees a higher stability for the glasses (TZ2 and TZ3), which had to undergo multiple collapsing steps, and thus prevents nucleation and growth of unwanted nanocrystals. The measured refractive index of the glasses was compatible with our design, being the refractive index of the core higher than the cladding one, corresponding to a numerical aperture (NA) of 0.32 between core and first cladding and a NA of 0.20 between the first and second cladding.

Fig. 1 shows the absorption spectra of TZ4 and TZ5 glasses in the infrared region. In the TZ5 absorption spectrum it is possible to distinguish the peak due to the Ce^{3+} transition from the $^2F_{5/2}$ ground state to the excited state $^2F_{7/2}$. Such peak is absent in the cerium free glass.

The spectra show a broad, strong absorption band between 2500 and 3500 cm^{-1} with the maximum at about 3000 cm^{-1}, attributed to the OH groups incorporated in the glass coming from the chemicals and the fabrication atmosphere [17]. The monitoring of the fiber diameter during fiber fabrication provided measured low spatial frequency long range diameter fluctuations to be of the order of ± 7 μm with respect to the average diameter value of 124 μm over a length of 150 m.

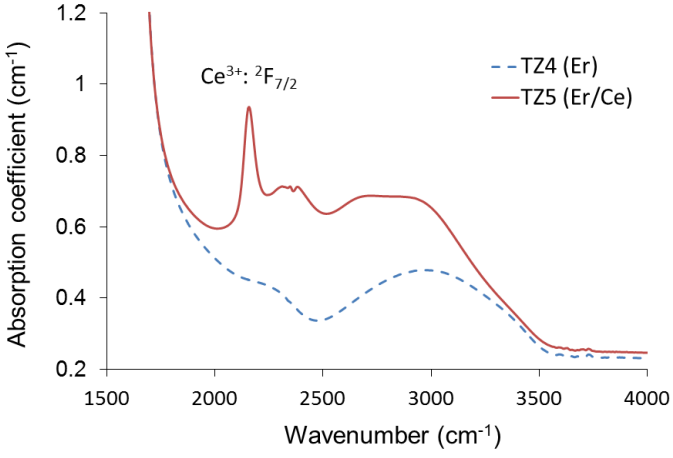

Fig. 1. FTIR absorption spectra of the Er^{3+} (TZ4) and Er^{3+}/Ce^{3+} (TZ5) co-doped tellurite glasses.

An optical micrograph of a section of the fabricated tellurite fiber is shown in Fig. 2, where the triple glass structure, featuring the Er^{3+}/Ce^{3+} doped glass composition TZ3 in the center, is clearly evident. In spite of the 6 □m diameter core being slightly out of center, the structure of the fiber was of good quality, free of major defects for the parts examined.

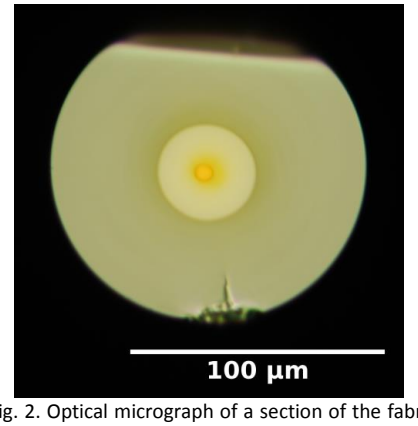

Fig. 2. Optical micrograph of a section of the fabricated tellurite fiber. The triple glass structure, featuring the Er^{3+}/Ce^{3+} doped glass composition TZ3 in the center, is clearly evident.

The near field imaging allowed us to determine that the fiber supported two modes, LP01 and LP11 at 1290 nm. The fiber attenuation loss measurements carried out on the initial, central and final stages of the drawing provided the values of 1.10 dB/m, 1.05 dB/m, and 1.00 dB/m at 1290 nm, respectively. The measurements used for the attenuation coefficient calculation are reported in Fig. 3. The standard deviation between fitted and measured values was ±0.05 dB/m. For clarity purpose the loss curve of the fiber for the initial stage of the drawing is not shown. The optical losses resulting from the butt-coupling at both end of the tellurite fiber were measured to be 6.4 dB.

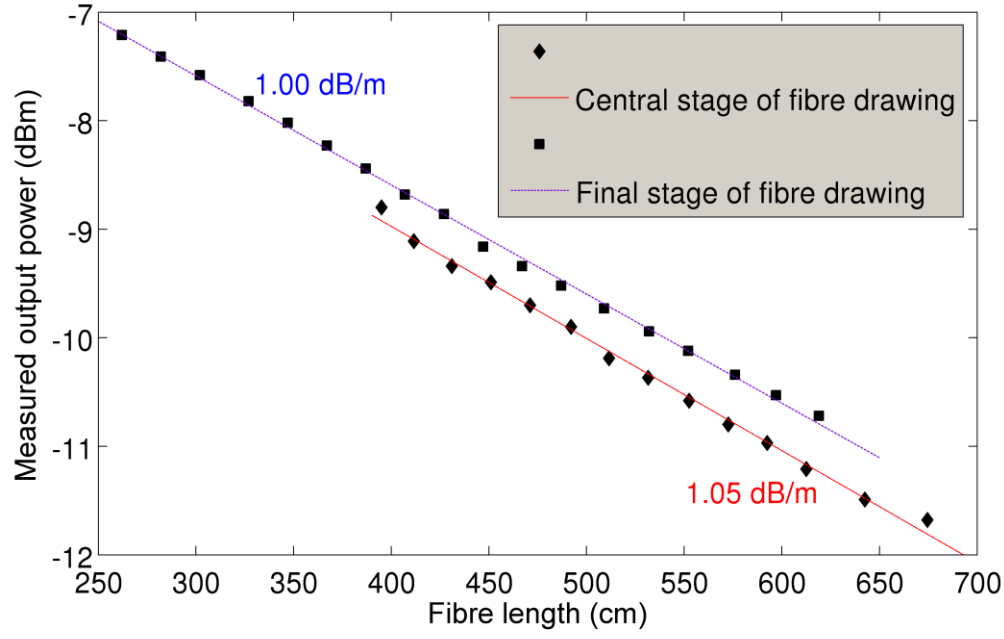

Fig. 3. Attenuation coefficient measurements performed by the cut-back method using a single mode optical fiber laser diode at 1.29 ?m.

3.2. Optical fiber laser demonstration

The coherent emission was successfully demonstrated and the spectrum of the laser is reported in Fig. 4. The output characteristics of the fiber laser are reported in Fig. 5. The maximum output power measured was 2.6 mW for a pump power of 250 mW at 976 nm, with threshold of around 100 mW. The corresponding slope efficiency of the laser was 1.3 % with respect to launched pump power. It is worth noting that strong green luminescence was easily seen with naked eyes in both experiments.

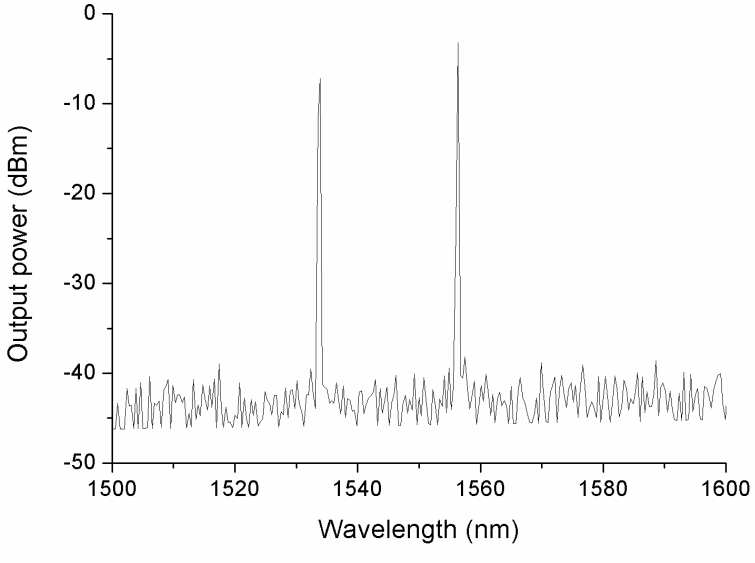

Fig. 4. Laser spectrum of the Er^{3+}/Ce^{3+} tellurite fiber obtained by exciting at the wavelength of 976 nm.

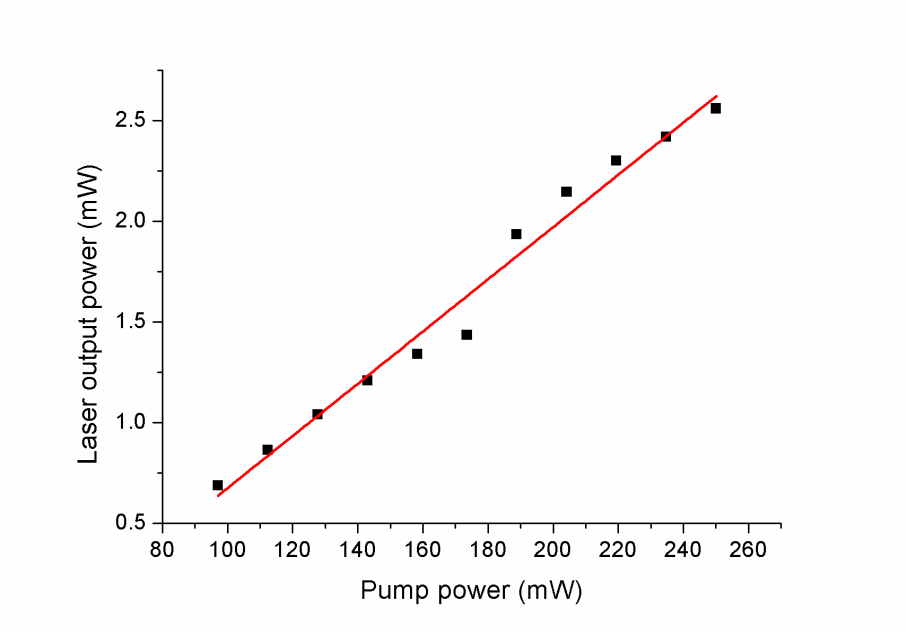

Fig. 5. 1.55 m output lasing power as a function of input pump power at 976 nm.

3.3. Optical fiber gain measurements

The signal net gain was measured for three signal input powers of -20 dBm, -10 dBm and 0 dBm at wavelength ranging from 1500 nm to 1640 nm. Results of measurements are shown in Fig. 6.

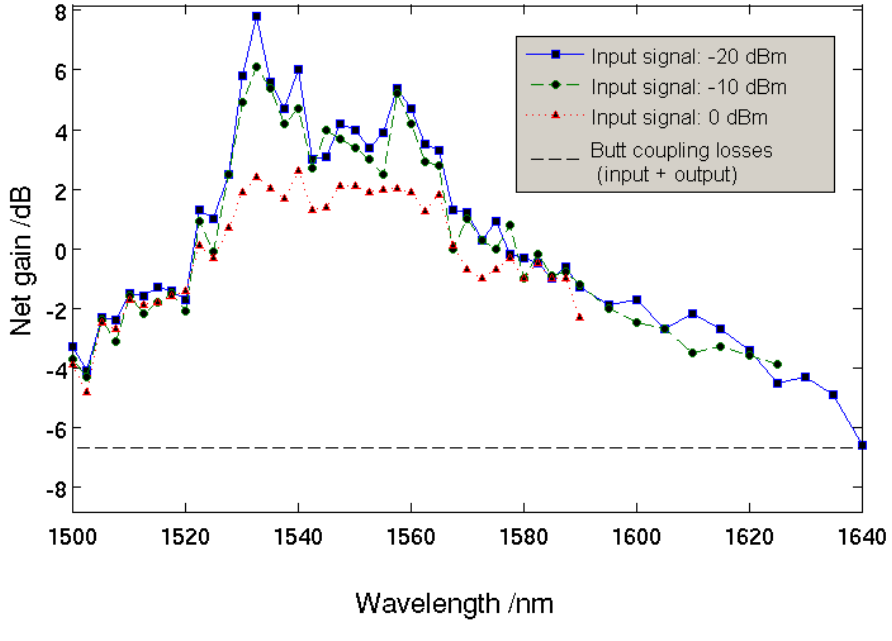

Fig. 6. The signal net gain measurement collected for three signal input powers of -20 dBm, -10 dBm and 0 dBm at wavelength ranging from 1500 nm to 1640 nm. Butt-coupling losses are also reported. Optical pump was 100 mW at 976 nm.

The intense visible green emission arising from the fiber suggests that in spite of the presence of Ce^{3+}, the pumping efficiency was still limited by upconversion mechanism. The green luminescence was showed to increase with increasing pump power. Nevertheless, net gain was achieved in the 10 cm long fiber for signal wavelength ranging from 1520 nm up to 1570 nm and signal power up to 0 dBm. Taking into account the coupling losses so as to consider internal gain rather than net gain, one can see that the wavelength for which the fiber effectively acts as an amplifier range from 1500 nm up

to about 1630 nm. Also, the fiber provided an internal gain as high as 14 dB for an input signal of -20 dBm at 1534 nm. Using a more adequate coupling technique, the net gain could reach this value.

3.4. Comparative luminescence spectra of Er and Er/Ce glass samples

TZ4 and TZ5 glasses, completely fabricated in the glove box, provided fluorescence spectra in the visible and near infrared wavelength range by pumping at 795 nm. To the naked eye the green upconversion luminescence appeared stronger for glass TZ5: a quantitative comparison between the two samples could not be possible due to unavoidable differences in the sample excitation configuration. In the case of infrared luminescence, both glasses, when pumped with the same intensity and in similar geometrical configuration, displayed emission peaks centered at 981 and 1533 nm corresponding to the $^4I_{11/2} \rightarrow {}^4I_{15/2}$ and $^4I_{13/2} \rightarrow {}^4I_{15/2}$ Er^{3+} transitions, respectively. The photoluminescence spectra are reported in Fig. 7.

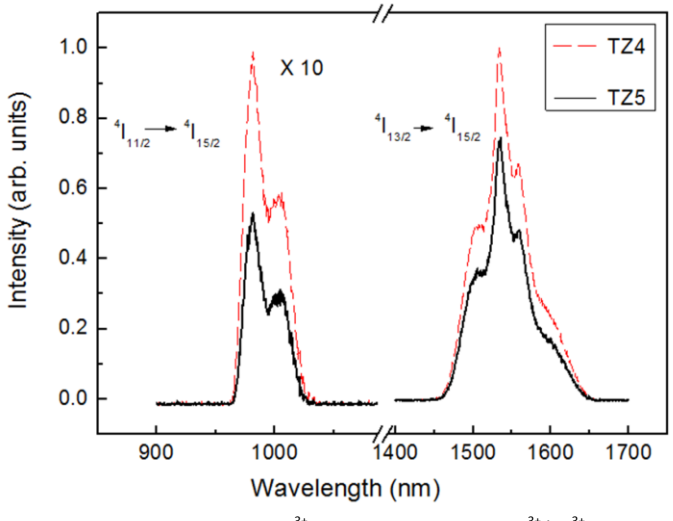

Fig. 7. Photoluminescence spectra of the Er^{3+} (TZ4) (dotted line) and Er^{3+}/Ce^{3+} (TZ5) (continuous line) activated tellurite glasses.

The lifetime values of Er^{3+}:$^4I_{13/2}$ and Er^{3+}:$^4I_{11/2}$ were measured at the wavelength of 1533 nm and 981 nm respectively, both by pumping at 795 nm and 514 nm. Results are reported in Table 2.

TABLE 2

Excited state lifetime values for Er^{3+} and Er^{3+}/Ce^{3+} doped samples by pumping at the wavelength of 795 nm and 514 nm respectively. The intensity ratio of the peaks at 1533 nm and at 981 nm is also reported for both glasses for comparison.

Glass label	N_{Er} (cm^{-3})	N_{Ce} (cm^{-3})	Er^{3+}:$^4I_{13/2}$ lifetime (ms) ±0.1ms		Er^{3+}:$^4I_{11/2}$ lifetime (ms) ±0.02ms		Intensity ratio[a] Er^{3+}
			@795 nm	*@514 nm*	*@795 nm*	*@514 nm*	*@795 nm*
TZ4 (Er)	$8.17 \cdot 10^{19}$	-	5.6	5.9	0.26	0.29	10.1
TZ5 (Er-Ce)	$8.12 \cdot 10^{19}$	$1.92 \cdot 10^{19}$	4.9	4.0	0.23	0.24	14.0

[a] Ratio between the lifetime values of the Er^{3+} ion decay levels $^4I_{13/2} \rightarrow {}^4I_{15/2}$/$^4I_{11/2} \rightarrow {}^4I_{15/2}$.

Excitation at 795 nm in $^4I_{9/2}$ state was performed in order to avoid possible site selection and any resonant excitation with the observed emitting state $^4I_{11/2}$. Evidence that site selection is negligible in these glasses is proved by the results reported in Table 2 where lifetimes were measured upon 514.5 nm and 795 nm excitation in the $^2H_{11/2}$ and $^4I_{9/2}$ states, respectively [18].

4. Discussion

Given the relatively low purity of the chemicals and the impossibility to develop the whole preform fabrication process inside a glove box, the quality of the fiber can be considered satisfying. It is worth mentioning that the passive tellurite glass fiber developed in our laboratory exhibits typical loss of 0.5 dB/m at 1.3 μm. The excess loss present in the Er/Ce doped fiber could be attributed to the tail of the absorption of Er3+, as suggested by Auzel [19]. Also possible contribution from tail band absorption due to OH contamination could be involved.

Regarding the supported modes, the numerical aperture value of 0.32 obtained from the refractive index measurements (see table 1) suggests that LP11 and LP12 modes should be supported, besides the observed LP01 and LP02. The origin of this discrepancy could be attributed to a mismatch of the thermo-mechanical properties between TZ1 and TZ2: the mechanical stress induced in the fiber might have reduced the NA of this latter. Such effect has been reported in several publications [20-23] in particular for glass systems with similar thermo-mechanical properties to tellurite glass such as fluoride glass. A higher control on numerical aperture of the fiber will be required if tellurite glass fiber is to form part of an optical component. This is particularly true in the case of an optical amplifier where the overlap of the signal field distribution with the pumped area plays a critical role in terms of performances. As shown in figure 3, the fiber losses range from 1.00 to 1.10 dB/m. This variation should be attributed to both error on measurements and possible fluctuations of quality between the section of fiber analyzed. These fluctuations can be due either to the presence of scattering centers or to short range fiber diameter variations. Although some improvements of the fiber fabrication process are being pursued, the diameter and loss data presented above suggest an acceptable level of reliability and reproducibility for the development of optical components at a research laboratory level.

The implementation of our tellurite glass fiber as a fiber laser performed better than previous fiber lasers obtained with similar configuration [7], being its slope efficiency double (1.3% vs 0.65%) and also reaching the same output power with a much shorter fiber: 10 cm in our case against 85 cm in [7].

Regarding the fiber implementation as an optical amplifier, our setup presents 8 dB maximum gain value, lower than that reported by Mori et al. [7], who measured up to 16 dB. Nonetheless it should be highlighted that the input signal used in this work was higher, being -20 dBm against -30 dBm in [7].

Taking into account the difference of fiber geometry, rare-earth ion concentration and device implementation, we therefore observed performances of the same order of magnitude as those reported by the NTT group. The same group reported a small signal gain value as high as 50 dB at 1560 nm wavelength, however the fiber length used was 14 m and the pumping scheme involved a 1480 nm laser diode as opposed to a 980 nm laser diode used in this work.

The green upconversion emission arising from the Er/Ce doped tellurite glass fiber when pumped at 980 nm suggests clearly that the low phonon energy characteristic of tellurite glass is not well adapted to standard telecom pumping schemes. This upconversion translates into a poor efficiency of the amplifier and laser in terms of energy: the slope efficiency was 1.3%.

Although a 1480 nm pumping scheme appears to be more efficient in limiting the detrimental upconversion effect, it would not allow reaching a sufficiently low noise figure value for the telecom industry. Nonetheless, other applications of Er doped tellurite glass fiber such as booster amplifier operating over a large bandwidth remain of interest if pumped using a 1480 nm laser source.

The presence of a strong green upconversion also highlights that the introduction of CeO_2 in the glass batch did not allow to quench the upconversion phenomena as reported in [11,24]. Actually the performances of the amplifier using tellurite glass fiber doped either with Er or Er/Ce are similar. This observation suggests that any possible enhancement of the performances thanks to the introduction of CeO_2 in the glass batch is limited.

The authors believe that introducing cerium as Ce^{4+} does not necessarily provide a correspondent amount of Ce^{3+} ions inside the glass host. In the case of fluoride glasses, Ce^{3+} is directly introduced through addition with CeF_3, whilst in the case of tellurite glasses CeO_2 is employed which is characterized by Ce^{4+}. Usually introduced into glass melts as an oxidizing agent [25], one could expect Ce^{4+} to reduce readily to Ce^{3+}. Indeed the absorption peak observed in Fig. 1 evidenced the presence of Ce^{3+} ions, though does not prove that all cerium is present as Ce^{3+}. Standard melting conditions of tellurite glass in oxidizing atmosphere cannot promote the reduction of Ce^{4+} to Ce^{3+}. It is therefore unlikely that all cerium compound is present as Ce4+. This assumption was validated by the strong green luminescence observed and by the measured gain values, which did not correspond to significant improvement if compared to cerium free tellurite optical fibers [7,8]. To further investigate the effect of cerium, two additional glasses TZ4 and TZ5 were fabricated and tested following the procedure presented by Choi et al. [11]. The results appeared quite different. The intensity peak ratio (table 2) increased with adding cerium ions, as reported in literature [11]. However, lifetime measurements demonstrated a shortening of Er^{3+}:$^4I_{13/2}$ lifetime and a substantially stable value of Er^{3+}:$^4I_{11/2}$ with adding Ce^{3+} ions which is unexpected considering the well-known cross-relaxation mechanism [12]. We believe that this behavior is due to a low amount of Ce^{3+}

in respect to Ce^{4+} in our fiber so that the cerium ions effect, leading to shortening of the $^4I_{11/2}$ level lifetime and enhancement of the emission intensity of the $^4I_{13/2}$?$^4I_{15/2}$ transition, is not observed.

Another important issue limiting as well the exploitation of tellurite glass fiber in real world systems concerns the packaging and implementation of tellurite glass fiber with other standard optical components. If compared to silica glass, tellurite is a fragile material [26,27] making difficult manipulating and handling tellurite glass fiber. For this reason, we suggest that the length of fiber to be used when tellurite glass is involved should be kept to a minimum. Indeed, this feature would be beneficial in terms of compactness and packaging. In this work, we have limited the implementation tasks to its most simple configuration so that coupling between standard silica fiber components and tellurite glass fiber was performed by butt-coupling, thus free of any kind of connectorization. This approach resulted in the rather high insertion losses of 3.2 dB. The NTT group reported losses as low as 0.3 dB using a titled V groove connection technique from a standard silica fiber to a 3 ?m core diameter fiber. Considering the mismatch between the two core diameters, one would not expect such low value. Actually, the insertion loss value reported by NTT is even lower than the typical insertion loss value of 0.4 dB that can be obtained using a standard angled connection of standard silica fibers. Considering the maturity of the later type of connector technology and the fact that it involves the same fiber diameters made from material of the same refractive index, the insertion loss reported by the NTT group seems intriguingly low.

Taking into account the dissimilarity between the two materials and the technological limitations involved in handling tellurite glass fiber, a minimum insertion loss value lower than 1dB appears difficult to achieve.

Again such insertion loss value is too high for the telecom industry, but could remain acceptable for more specific applications. Further work should take into account the possibility of introducing cerium ions as CeF_3, in the attempt to minimize cerium oxidation during melting and processing the glass.

5. Conclusions

The results presented in the paper highlight several limitations for what concerns the application of erbium doped tellurite glass fiber for the manufacture of telecom optical amplifier. The low phonon energy of tellurite glass does not match with existing telecom components and technologies. To date, the advantages in developing a specific technology to exploit tellurite glass fibers are unclear and unlikely to be ever commercially viable. The above comments can be extended more generally to the exploitation of other soft glass fiber such as fluoride or chalcogenide glass fibers.

In spite of the limitations mentioned, the results reported here and those of previous work suggest that tellurite glass fibers perform well in particular in terms of amplification bandwidth. Moreover, their high rare-earth solubility allows the development of compact fiber components.

Further improvements of the amplifier efficiency are nonetheless necessary. The use of Ce^{3+} to overcome the low phonon energy limits of tellurite glass could be a reliable approach but as our results suggest a careful control of the melting redox conditions is required. This is true whether cerium is introduced as Ce^{3+} or Ce^{4+}. An alternative and perhaps more direct approach relies in developing a tellurite glass matrix with a higher phonon energy without impairing on the amplification bandwidth.

By means of these improvements, compact erbium doped tellurite glass fiber amplifier and laser could be implemented in particular for developing novel sources in the eye safe region around 1.5 ?m.

From our results we could conclude that most part of Ce^{4+} ions was not reduced to Ce^{3+} during glass fabrication and thus did not provide the expected effect on erbium emission, at least in the case of our glass fabrication procedure. Further research activity should be focused on adding Ce^{3+} as batch reagent and thus assess the difference with the samples displayed in this work.

Acknowledgements

The authors acknowledge the invaluable technical assistance of E. Moser (University of Trento), A. Carpentiero (IFN-CNR), and S. Varas (IFN-CNR).

References

[1] R. Paschotta, *Encyclopedia of Laser Physics and Technology*. Berlin: Wiley-VCH, 2008.

[2] J.S. Wang, E.M. Vogel, E. Snitzer "Tellurite glass: a new candidate for fiber devices", *Opt. Mat.*, vol. 3, pp. 187-203, Aug. 1994.

[3] L. Le Neindre, S. Jiang, B.C. Hwang, T. Luo, J. Watson, N. Peyghambarian, "Effect of relative alkali content on absorption linewidth in erbium-doped tellurite glasses", *J. Non-Cryst. Sol.*, vol. 255, no. x, pp. 97-102, Sept. 1999.

[4] H. Gebavi, D. Milanese, R. Balda, S. Chaussedent, M. Ferrari, J. Fernandez, and M. Ferraris, "Spectroscopy and optical characterization of thulium doped TZN glasses", *J. Phys. D: Appl. Phys.*, vol. 43, no. xx, pp. 135104 - 1/8, Mar. 2010.

[5] S. Tanabe, N. Sugimoto, S. Ito, T. Hanada, "Broad-band 1.5 μm emission of Er^{3+} ions in bismuth-based oxide glasses for potential WDM amplifier", *J. Lumin.*, vol. 87-89, pp. 670-672, May 2000.

[6] R. Rolli, M. Montagna, S. Chaussedent, A. Monteil, V.K. Tikhomirov, M. Ferrari, "Erbium-doped tellurite glasses with high quantum efficiency and broadband stimulated emission cross section at 1.5 μm", *Opt. Mat.*, vol. 21, no. 4, pp. 743-748, Feb. 2003.

[7] A. Mori, Y. Ohishi, and S. Sudo, "Erbium-doped tellurite glass fibre laser and amplifier," *Electron. Lett.*, vol. 33, no. 10, pp. 863-864, May 1997.

[8] A. Mori, K. Kobayashi, M. Yamada, T. Kanamori, K. Oikawa, Y. Nishida, and Y. Ohishi, "Low noise broadband tellurite-based Er^{3+}-doped fiber amplifiers", *Electron. Lett.*, vol. 34, no. 9, pp. 887-888, Apr. 1998.

[9] A. Mori, T. Sakamoto, K. Kobayashi, K. Shikano, K. Oikawa, K. Hoshino, T. Kanamori, Y. Ohishi, and M. Shimizu, "1.58□m Broad-Band Erbium-Doped Tellurite Fibre Amplifier", *IEEE J. Light. Tech.*, vol. 20, no. 5, pp.794-799, May 2002.

[10] Z. Meng, T. Yoshimura, K. Fukue, and M. Higashihata, "Large improvement in quantum fluorescence yield of Er^{3+}-doped fluorozirconate and fluoroindate glasses by Ce^{3+} codoping," *J. Appl. Phys.*, vol. 88, no. 5, pp. 2187-2190, Sept. 2000.

[11] Y.G. Choi and K.H. Kim, S.H. Park and J. Heo, "Comparative study of energy transfers from Er^{3+} to Ce^{3+} in tellurite and sulfide glasses under 980 nm excitation", *J. Appl. Phys.*, vol. 88, no. 7, pp. 3832-3839, Oct. 2000.

[12] M. Mattarelli et al., "Effect of Eu^{3+} and Ce^{3+} codoping on the relaxation of Er^{3+} in silica-hafnia and tellurite glasses" *Phys. Stat. Sol.*, vol. 4, no. 3, pp. 793-796, Mar. 2007.

[13] F. Auzel and P. Goldner, "Towards rare-earth clustering control in doped glasses", *Opt. Mat.*, vol. 16, no. x, pp. 93-103, Feb./Mar. 2001.

[14] S. Dai, C. Yu, G. Zhou, J. Zhang, G. Wang, and L. Hu, "Concentration quenching in erbium-doped tellurite glasses", *J. Lumin.*, vol. 117, no. 1, pp. 39-45, Mar. 2006.

[15] R. Balda, J. Fernández, S. García-Revilla, and J. M. Fernández Navarro, "Spectroscopy and concentration quenching of the infrared emissions in Tm^{3+}-doped TeO_2-TiO_2-Nb_2O_5 glass", *Opt. Expr.*, vol. 15, no. x, pp. 6750-6761, May 2007.

[16] R. I. Laming, M. C. Farries, P. R. Morkel, L. Reekie, D. N. Payne, P. L. Scrivener, F. Fontana, and A. Righetti, "Efficient pump wavelengths of erbium-doped fibre optical amplifier", *Electron. Lett.*, vol. 25, no. 1, pp. 12-14, Jan. 1989.

[17] S. Dai, C. Yu, G. Zhou, J. Zhang, G. Wang, "Effect of OH^- content on emission properties in Er^{3+}-doped tellurite glasses", *J. Non-Cryst. Sol.*, vol. 354, no. 12-13, pp. 1357-1360, Feb. 2008.

[18] G.C. Righini and M. Ferrari, "Photoluminescence of rare-earth-doped glasses", *Riv. Nuovo Cimento*, vol. 28, no. 10, pp. 1-53, Sept. 2005.

[19] F. Auzel, "Existence of intrinsic background drawbacks and usefulness", *Electron. Lett.*, vol.29, no. 4, pp. 337-338, Feb. 1993.

[20] Nakai, N. Norimatsu, Y. Nods, O. Shinbori, and Y. Mimura "Changes in refractive index of fluoride glass fibers during fiber fabrication processes" Appl. Phys. Lett. 56 (3), 15 January 1990

[21] P. K. Bachmann, W. Hermann, H. Wehr, and D. U. Wiechert "Stress in optical waveguides. 2: Fibers" Applied Optics, Vol. 26, Issue 7, pp. 1175-1182, Apr. 1987.

[22] G. W. Scherer, A. R. Cooper, "Thermal Stresses in Clad-Glass Fibers", J. Amer. Ceram. Soc. Volume 63, Issue 5-6, pages 346–347, May 1980

[23] U. C. Paek, C. R. Kurkjian, "Calculation of Cooling Rate and Induced Stresses in Drawing of Optical Fibers", J. Amer. Ceram. Soc., Volume 58, Issue 7-8, pages 330–335, July 1975

[24] S. Shen, L. Huang, P. Joshi, and A. Jha, "Gain characteristics of Er^{3+}/Ce^{3+} codoped tellurite short fibre amplifier pumped at 980 nm", *Electron. Lett.*, vol. 39, no. 25, pp. 34-35, Dec. 2003.

[25] V.V. Vargin, G.A. Osadchaya, "Cerium dioxide as a fining agent and decolorizer for glass", *Glass Ceram.*, vol. 17, no. 2, pp. 78-82, Dec. 1960.

[26] R.A.H. El-Mallawany, *Tellurite Glasses Handbook.* Boca Raton: CRC Press, 2002.

[27] R. Stepien, R. Buczynski, D. Pysz, I. Kujawa, M. Mirkowska, "Tellurite glasses for microstructured optical fibres manufacturing", *Photon. Lett. Pol.*, vol. 2, no. 1, pp.16-18, Mar. 2010.